Rhenium(VI)-oxidephosphate: Chemical Vapour Transport, Crystal Structure, Spectroscopic Characterization and Magnetic Behaviour

Robert Glaum, Saiful M. Islam

Zeitschrift für Anorganische und Allgemeine Chemie

Rhenium(VI)-oxidephosphate: Chemical Vapour Transport, Crystal Structure, Spectroscopic Characterization and Magnetic Behaviour

Journal:	*Zeitschrift für Anorganische und Allgemeine Chemie*
Manuscript ID:	zaac.200900066
Wiley - Manuscript type:	Article
Date Submitted by the Author:	23-Jan-2009
Complete List of Authors:	Glaum, Robert; Rheinische Friedrich-Wilhelms-Universitaet, Institut fuer Anorg. Chemie Islam, Saiful M.; Rheinische Friedrich-Wilhelms-Universitaet, Institut fuer Anorg. Chemie
Keywords:	Rhenium, Chemical vapor transport

Contributions on thermal behaviour and crystal chemistry of anhydrous phosphates. XXXXIII [1]

Rhenium(VI)-oxidephosphate: Chemical Vapour Transport, Crystal Structure, Spectroscopic Characterization and Magnetic Behaviour

S. M. Islam [2] and R. Glaum [1]

Received:.....

Dedicated to Professor G. Meyer on the occasion of his 60th birthday.

Bonn, Institut für Anorganische Chemie der Rheinischen Friedrich-Wilhelms-Universität

Abstract. $Re_2O_3(PO_4)_2$ was obtained as microcrystalline, dark-red powder at 450°C by reaction of ReO_3 with P_4O_{10}. Crystallization was achieved via chemical vapour transport in a temperature gradient 600 → 500 °C using iodine as transport agent. $Re_2O_3(PO_4)_2$ (*Pmcn*, Z = 4, a = 6.2986(6) Å, b = 7.79654(5) Å, c = 15.2714(12) Å), 86 parameters, 1185 independent reflections, R_1 = 0.027, wR_2 = 0.066) adopts its own structure type. The crystal structure consists of isolated double-octahedra [$Re^{VI}_2O_{11}$] and [PO_4] tetrahedra.

$Re_2O_3(PO_4)_2$ shows a weak temperature dependent magnetic moment ($0.05 \le \mu_{exp}/\mu_B \le 0.27$; 3 K ≤ T ≤ 300 K). Its single-crystal electronic absorption spectrum exhibits a weak band around

[1] Prof. Dr. R. Glaum
Institut für Anorganische Chemie, Uni Bonn
Gerhard-Domagk-Straße 1
D-53121 Bonn
e-mail: rglaum@uni-bonn.de

$\tilde{\nu}$ = 12000 cm^{-1}, above $\tilde{\nu}$ = 16000 cm^{-1} the UV/vis spectrum is completely dark.

Keywords: rhenium, chemical vapour transport, crystal growth, d^1 systems, electronic structure, crystal structure

Introduction

Molybdenum and tungsten are well known for the large number of anhydrous phosphates formed by these metals. In the ternary system Mo/P/O eight phosphates are known up to now $(Mo^{VI}O_2)_2(P_2O_7)$ [3], $(Mo^{VI}O_2)(PO_3)_2$ [4], $Mo^{V}OPO_4$ [5], $(Mo^{V}O)_4(P_2O_7)_3$ [6], $(Mo^{V}O)_2P_4O_{13}$ [7], $Mo_{1.3}O(P_2O_7)$ [8], $Mo^{IV}P_2O_7$ [9], and $Mo^{III}(PO_3)_3$ [10]. In case of tungsten $W^{VI}{}_2O_3(PO_4)_2$ [11, 12], $W^{VI}OP_2O_7$ [13], $W^{V}OPO_4$ [14], $W^{V}{}_2O_3(P_2O_7)$ [15], and $W^{IV}P_2O_7$ [16] are known. In addition, there is a large number of mixed valence $W^{V/VI}$ oxide phosphates, so called monophosphate tungsten bronzes, with general formula $(PO_2)(WO_3)_{2m}$ ($2 \leq m \leq 14$) [17]. As characteristic structural feature these bronzes contain ReO_3-type slabs separated by phosphate groups [17]. The large number of phosphates formed by molybdenum and tungsten is due to their stabilization in several oxidation states. The phase relations in the ternary systems Mo/P/O and W/P/O have been investigated some years ago [6, 18, 19]. For rhenium, on the other hand, despite its diagonal relationship to molybdenum, and its neighbourhood to tungsten, up to now just one phosphate, $Re^{IV}P_2O_7$, is described in literature [20, 21]. By judging from the number of binary rhenium oxides (ReO_2 [22], ReO_3 [23], $Re_{1.16}O_3$ [24], Re_3O_{10} [25], Re_2O_7 [26]) one clearly should expect further anhydrous rhenium phosphates in addition to ReP_2O_7. This lack in information on such compounds inspired us to search for new rhenium phosphates.

Our interest in these phosphates intensified since they might exhibit various properties that make them attractive materials, especially as heterogenous catalysts for selective oxidation of light alkanes [27]. Compounds containing V^{IV}, V^{V}, Mo^{V}, Mo^{VI}, and W^{VI}, all with metal-oxygen double bonds $(M{=}O)^{n+}$, are among the most active catalysts for such reactions (e.g.: $(VO)_2P_2O_7$ [28]). Actually, in theoretical studies the catalytic activity of these compounds is related to the presence of $(M{=}O)^{n+}$ at the materials surface, allowing transfer of oxygen to the hydrocarbon [29]. In addition to vanadium, molybdenum and tungsten, rhenium bears the capability of forming $(Re{=}O)^{n+}$ groups.

According to literature, electronic spectra and magnetic behaviour of the compounds of 5d elements are not well characterized. In this paper we report on synthesis, crystallization, structure, electronic absorption spectrum and magnetic behaviour of rhenium(VI)-oxide phosphate $Re_2O_3(PO_4)_2$.

Experimental Section

Syntheses. Microcrystalline powders of $Re_2O_3(PO_4)_2$ were obtained by isothermal heating in sealed silica tubes ($l \approx 11$ cm, $d \approx 1.5$ cm, $V \approx 20$ cm^3) of ReO_3 and P_4O_{10} (eq. 1) or via reduction of Re_2O_7 by red phosphorus in the presence of P_4O_{10} (eq. 2). ReO_3 was synthesized according to literature [30, 31]. Re_2O_7 and P_4O_{10} were handled in a glove bag in argon atmosphere since both materials are hygroscopic. The starting materials were at least of p.a. grade. The reactions were always conducted in two steps, i.e. prereaction by mild heating with a Bunsen burner and subsequent heating, keeping the starting materials at 450 °C in a two zone furnace, with the other end of the tube at 550 °C. Iodine (≈32 mg) was used as mineralizer. To get a single phase product approximately 40% more P_4O_{10} and 20% less red phosphorus with respect to the stoichiometry of $Re_2O_3(PO_4)_2$ were used. At about 700 °C, the reaction aiming for $Re_2O_3(PO_4)_2$ led to ReP_2O_7 (eq. 3a). Even without phosphorus as reductand ReO_3, $Re_2O_3(PO_4)_2$, and ReP_2O_7 exist in equilibrium besides O_2(g) at all temperatures in the range 450°C ≤ T ≤ 650°C (eq. 3b). Reaction of Re_2O_7 and P_4O_{10} at T ≤ 450°C led to the formation of pale-yellow crystals "$RePO_6$" with yet unknown structure. Its XRD powder pattern is shown in Fig. 1. A summary of representative experiments on synthesis, thermal behaviour and CVT of $Re_2O_3(PO_4)_2$ is given in Table 1.

$$4\ ReO_3 + P_4O_{10} \rightarrow 2\ Re_2O_3(PO_4)_2 \quad (1)$$

$$5\ Re_2O_7 + 2\ P + 2\ P_4O_{10} \rightarrow 5\ Re_2O_3(PO_4)_2 \quad (2)$$

$$2\ Re_2O_7 + P_4O_{10} \rightarrow 2\ ReO_3 + 2\ ReP_2O_7 + 2\ O_2(g) \qquad (T \geq 700°C) \quad (3a)$$

$$2\ Re_2O_7 + P_4O_{10} \rightarrow 2\ Re_2O_3(PO_4)_2 + O_2(g) \qquad (450°C \leq T \leq 650°C) \quad (3b)$$

$$2\ Re_2O_7 + P_4O_{10} \rightarrow 4\ \text{“}ReO_2(PO_4)\text{”} \qquad (T \leq 450°C) \qquad (3c)$$

The crystallization of $Re_2O_3(PO_4)_2$ was achieved by chemical vapour transport (CVT) in sealed silica tubes ($l \approx 11$ cm, $d \approx 1.5$ cm, $V \approx 20$ cm ^{3}), which were placed in the temperature gradient of electrically heated two zone furnaces. Fig. 2 shows crystals of $Re_2O_3(PO_4)_2$ obtained by CVT. A summary of representative experiments on synthesis, thermal behaviour and CVT of $Re_2O_3(PO_4)_2$ is given in Table 1.

Characterization

Energy-dispersive x-ray fluorescence analyses [32, 33] (EDAX system, scanning microscope DMS 940, Zeiss) showed no additional elements besides rhenium, phosphorus and oxygen.

For identification, examination of the purity, and for determination of the lattice parameters of $Re_2O_3(PO_4)_2$ image-plate **(*IP*) Guinier photographs** (Guiner camera FR-552 Enraf-Nonius, quartz-monochromator, Cu-Kα_1 radiation, λ = 1.54052 Å, α-SiO_2 as internal standard, BAS-TR 2025 image plate film (Fa. Fuji), BAS-1800 scanner (Fa. Fuji), software: BASReader [34], AIDA [35] for digitization) [36, 37, 38] were taken. Assignment of the powder pattern led to a = 6.2986(6) Å, b = 7.7965(6) Å, c = 15.271(1) Å (78 reflections with $32.47° \leq 4\theta \leq 124.99°$).

Single-crystal x-ray study. Intensity data were measured on a κ-CCD diffractometer (Enraf-Nonius Inc.) at ambient temperature. Structure determination and refinement was performed using the SHELX-97 [39] suite in the WinGX framework [40].

Details concerning data collection, structure solution and refinement of $Re_2O_3(PO_4)_2$ are summarized in Table 2. The final atomic coordinates and displacements parameters are reported in Table 3. Selected interatomic distances and angles are listed in Table 4. A crystallographic information file containing also lists of the complete interatomic distances and angles were deposited at FIZ (CSD-420290). Copies are available at:

Fachinformationszentrum Karlsruhe, Abt. IDNT, D-76344 Eggenstein-Leopoldshafen (e-mail: crysdata@fiz-karlsruhe.de).

The ***electronic absorption spectrum*** (Fig. 3) of a single crystal of $Re_2O_3(PO_4)_2$ (0.1 0.05 0.02 mm^3) was measured at ambient temperature using a strongly modified CARY 17 microcrystal spectralphotometer (spectral services, ANU Canberra, Australia [41 42]). The spectrometer allows measurement of polarized absorption spectra of very small single crystals with diameters down to 0.1 mm in the UV/vis/nir range (36000 $cm^{-1} \geq \tilde{\nu} \geq 5800\ cm^{-1}$). Details on the spectrometer have already been reported [37, 38]. The spectrum shows one weak absorption at $\tilde{\nu} = 12000\ cm^{-1}$. Above $\tilde{\nu} = 16000\ cm^{-1}$ all light is absorbed by $Re_2O_3(PO_4)_2$.

Vibrational spectra of $Re_2O_3(PO_4)_2$ (Fig. 4) were measured on a FT-IR (IFS 113v, BRUKER) and on a FT-Raman spectrometer (RFS 100, BRUKER). For IR investigations tablets of the phosphate dispersed in KBr were used. For the Raman spectrum the pure material was used.

Magnetic susceptibility of $Re_2O_3(PO_4)_2$ (Figure 5) as a function of temperature was measured in a Quantum Design Physical-Property-Measurement-System (Institut für Anorganische und Analytische Chemie, Uni Münster) in the temperature range 3 - 300 K with magnetic flux densities up to 80 kOe. The sample was packed in kapton foil and attached to the sample holder rod of the VSM. The susceptibility χ_{corr} given in Figure 5 is corrected for the diamagnetic contribution of the core electrons. Based on the diamagnetic susceptibilities $\chi_{dia}(Re^{6+}) = -16\cdot10^{-6}$ mol/cm^3, $\chi_{dia}(O^{2-}) = -12\cdot10^{-6}$ mol/cm^3, and $\chi_{dia}(PO_4^{3-}) = -47\cdot10^{-6}$ mol/cm^3 [43, 44, 45] the correction $\chi_{dia}(Re_2O_3(PO_4)_2) = -162\cdot10^{-6}$ mol/cm^3 was estimated. Using $\mu_{exp}/\mu_B = 2.8279\cdot(T\cdot\chi_{mol})^{1/2}$ the magnetic moment per Re^{6+} ion (Figure 5) was calculated.

Results and Discussion

Synthesis and crystallization. In contrast to most other transition metal phosphates, for $Re_2O_3(PO_4)_2$ and most other rhenium phosphates, both, thermal reduction as well as thermal decomposition into $P_4O_{10}(g)$ is observed already at temperatures as low as 450°C. Thus, synthesis of rhenium phosphates, others than ReP_2O_7, requires precise control of $p(O_2)$, $p(P_4O_{10})$, and temperature. The empirically optimized experimental conditions for the synthesis of $Re_2O_3(PO_4)_2$ indicate that the rhenium(VI) oxide phosphate is stable at T > 500°C only in equilibrium with considerable pressures $p(O_2)$ and $p(P_4O_{10})$.

Due to the limited thermal stability of $Re_2O_3(PO_4)_2$ and the high volatility of $ReO_3I(g)$ and $P_4O_{10}(g)$ the method of chemical vapour transport (CVT) [46] works nicely for crystallization of the oxide phosphate. Migration proceeds from higher to lower temperature ($T_2 \rightarrow T_1$, $T_2 > T_1$, $\Delta T \approx 100$ °C) due to endothermic reactions (Table 1). Phosphorus forms various volatile oxides P_4O_n, $6 \leq n \leq 10$, PO_g and $PO_{2,g}$. Among them $P_4O_{10,g}$ seems to be the most important species for the transport of phosphorus due to its already known thermodynamic stability [19, 47] under the given (oxidizing) conditions. The stability and importance of gaseous ReO_3X (X = OH, I) for CVT of rhenium oxides has been discussed in detail [30]. Hence, CVT of $Re_2O_3(PO_4)_2$ is expected to proceed according to reaction 4. In our experiments P_4O_{10}, which is hygroscopic, was used as a starting material, so we may expect the presence of small amounts of water in the ampoules. Due to hydrolysis of $ReO_3I(g)$ and $P_4O_{10}(g)$ reactions (5) and (6) are expected to contribute to the composition of the gas phase. While very slow CVT of ReO_3 was observed [30] using water as transport agent, migration of $Re_2O_3(PO_4)_2$ in a temperature gradient with water as transport agent was not observed (Table 1).

$$Re_2O_3(PO_4)_2(s) + I_2(g) \rightarrow 2\ ReO_3I(g) + {}^1/_2\ P_4O_{10}(g) \quad (4)$$

$${}^n/_4\ P_4O_{10}(g) + {}^n/_2\ H_2O(g) \rightarrow (HPO_3)_n(g) \qquad (n = 1, 3, 4) \quad (5)$$

$$2\ ReO_3I(g) + H_2O(g) \rightarrow 2\ ReO_3OH(g) + 2\ HI(g) \quad (6)$$

Crystal Structure. While $[Re_2O_{10}]$ groups and $[ReO_6]$ octahedra in various degrees of condensation are frequently encountered in the crystal chemistry of oxo-rhenates [48], isolated $[Re_2O_{11}]$ units were hitherto unknown. In the crystal structure of rhenium(VI) oxide-phosphate, $Re_2O_3(PO_4)_2$, double-octahedra $[Re_2O_{11}]$ and $[PO_4]$ tetrahedra are forming chains running parallel to the crystallographic *c*-axis (Figure 6). These are linked to four adjacent chains via the phosphate groups only. There are no direct links via oxygen atoms from one $[Re_2O_{11}]$ group to another. Despite the same space group and very similar lattice parameters, the orthorhombic modification of $W_2O_3(PO_4)_2$ [12] is not immediately structurally related to rhenium(VI) oxide-phosphate. The structure of the vanadate $Re_2V_2O_{11}$ is up to now not determined reliably [49].

The Re^{6+} ions in $Re_2O_3(PO_4)_2$ show a distorted octahedral coordination by oxygen atoms with 1.66 Å ≤ *d*(Re-O) ≤ 2.07 Å (Fig. 7, Table 4). Four oxygen ligands are provided by phosphate groups. The coordination sphere of Re1 and Re2 is completed by one oxygen atom bridging between two rhenium atoms ($d(Re\text{-}O_b) \approx 1.84$ Å) and by one terminal oxygen atom per rhenium ($d(Re\text{-}O_t) \approx 1.66$ Å). The latter distance might be interpreted as $(Re{=}O)^{4+}$ group, a structural feature so far unobserved for oxo-compounds of hexavalent rhenium. In agreement with literature data for dinuclear rhenium(V) coordination compounds of the type $Re_2O_3L_8$ [50] signals in the Raman spectrum (Fig. 4) observed around 970 cm^{-1} are assigned to ν(Re=O).

The phosphate groups have a geometric structure close to an ideal tetrahedron, with all oxygen atoms coordinated to just one rhenium (Table 4).

Electronic Structure. Due to the low symmetry of the ligand-field around the Re^{6+} ions and the strong interaction between rhenium and the double-bonded oxygen a quantitative treatment of the Re^{6+} d-electron states was not attempted. The rather low magnetic moment observed for Re^{6+} in $Re_2O_3(PO_4)_2$ ($0.05 \leq \mu_{exp}/\mu_B \leq 0.27$; 3 K ≤ *T* ≤ 300 K; Fig. 5) and its strong temperature dependence are indicative for strong spin-orbit coupling, as expected for a

5d transition metal. In addition, the temperature dependence might be a consequence of the low-symmetry ligand field. We relate the absorption band observed around $\tilde{\nu}$ = 12000 cm^{-1} (Fig. 3) to a d-d electronic transition, due to its rather low absorbance. The strong absorption above $\tilde{\nu}$ = 16000 cm^{-1} is likely to originate from a charge transfer transition $O^{2-} \rightarrow Re^{6+}$. Whether additional d-d transitions at higher wavenumbers are thus obscured remains unclear. Further investigations on the elctronic structure of rhenium in various oxidation states stabilites in anhydrous phosphates are ongoing.

Conclusions

Our study shows that CVT experiments with iodine as transport agent are particularly suitable for the crystallization of thermally labile rhenium phosphates. The first single-crystal structure investigation of an anhydrous rhenium phosphate revealed unprecedented isolated di-octahedral $[Re^{VI}_2O_{11}]$ groups with two terminal (Re=O) bonds as building units besides phosphate tetrahedra. Even so $Re_2O_3(PO_4)_2$ shows some crystal chemical similarities to anhydrous tungsten phosphates, its redox behaviour is distinctly different.

Acknowledgement

We thank W. Hermes and Prof. Dr. R. Pöttgen (Univ. Münster) for the magnetic measurement of $Re_2O_3(PO_4)_2$ as well as Dr. J. Daniels and Prof. Dr. J. Beck (Univ. Bonn) for the collection of the single-crystal data. S. I. is grateful to DAAD for a scholarship. This work was supported by Deutsche Forschungsgemeinschaft (grant GLA 259/3-1,2).

Table 1 Experiments for synthesis and chemical vapour transport of $Re_2O_3(PO_4)_2$.

starting materials / mg		I_2 / mg	temperatures[a] / °C	time / h	products(source) (according to Guinier photographs)	products(sink)
ReO_3	112.2	30	400 → 500	96		
P_4O_{10}	67.1		500 → 400	240		no transport
			600 → 500	240	ReP_2O_7 / $Re_2O_3(PO_4)_2$	$Re_2O_3(PO_4)_2$ / ReP_2O_7
ReO_3	183.9	48	B. B.[b]	4		
P_4O_{10}	74.1		550 → 650	120		no transport
			600 → 500	216	ReO_3 / $Re_2O_3(PO_4)_2$ / ReP_2O_7	$Re_2O_3(PO_4)_2$ / ReO_3 / ReP_2O_7
ReO_3	197.9	57	B. B.	1		
P_4O_{10}	59.9		550 → 650	120		no transport
			600 → 500	216	ReO_3 / ReP_2O_7 / $Re_2O_3(PO_4)_2$	ReO_3 / ReP_2O_7 / $Re_2O_3(PO_4)_2$
ReO_3	253.1	50	B. B.	3.5		
P_4O_{10}	97.2		500 → 550	170		no transport
			600 → 500	240	ReP_2O_7 / $Re_2O_3(PO_4)_2$	$Re_2O_3(PO_4)_2$ / ReP_2O_7
$Re_2O_3(PO_4)_2$	120.0	24	500 → 400	120		no transport
			600 → 500	168	$Re_2O_3(PO_4)_2$/ ReP_2O_7	no transport
$Re_2O_3(PO_4)_2$	132.4	---	450	216	$Re_2O_3(PO_4)_2$	no transport
Re_2O_7	571.5	32	600 → 700	96		no transport
P_4O_{10}	133.9		700 → 600	144	ReP_2O_7	ReP_2O_7 / $Re_2O_3(PO_4)_2$
P	12.4					
Re_2O_7	350.2	---	300 → 400	168		
P_4O_{10}	104.6		400 → 300	192	yellow crystals ("$RePO_6$")	yellow crystals ("$RePO_6$")
Re_2O_7	353.8	---	300 → 400	96		
P_4O_{10}	101.6		400 → 300	192		
			450 → 350	144	yellow crystals ("$RePO_6$")	yellow crystals ("$RePO_6$")
Re_2O_7	378.0	40	B. B.	~0.2		
P_4O_{10}	89.73		450	72		no transport
P	9.71		450 → 500	120	$Re_2O_3(PO_4)_2$/ReO_3	
Re_2O_7	255.7	47	B. B.	3		
P_4O_{10}	85.1		450 → 550	144	$Re_2O_3(PO_4)_2$	------
P	5.1					

[a] Given are the various heating periods for an ampoule. Starting solid always at the temperature at the left side of the arrow. Solid reaction products were characterized by their XRPD pattern after the final heating period, only.

[b] B. B.: mild heating in the bunsen burner flame

Table 2 $Re_2O_3(PO_4)_2$. Crystallographic data, structure solution and refinement.

Chemical formula	$Re_2O_3(PO_4)_2$
Formula weight (g/mol)	610.35
Crystal system	orthorhombic
Space group	*Pmcn (no. 62)*
a	6.2986 (6) Å
b	7.7965 (6) Å
c	15.2714 (12) Å
V	749.93(11) $Å^3$
Z	4
D_{calc} (g/cm³)	5.406
Radiation, wavelength, monochromator	MoK_α (λ = 0.71073 Å), graphite
μ (mm^{-1})	32.74
Colour	dark red crystal, reddish powder
Diffractometer	κ-CCD (NONIUS)
Crystal size	~ 0.2 · 0.2 · 0.1
F(000)	1072.0
Temperature	293 K
Theta range/ °	$0.998 \leq \theta \leq 30.034$
Collected reflections	20576
Independent reflections	1185
Index ranges (whole sphere)	$-8 \leq h \leq 8$ $-10 \leq k \leq 10$ $-21 \leq l \leq 21$
No. of parameters used	86
R_1/wR_2 (for all data)	0.027 / 0.066
Goof on F^2	1.234
weighting scheme	$w = 1/[\sigma^2(F_o^2) + (0.0208P)^2 + 11.98P]$, where $P = (F_o^2+2F_c^2)/3$

Table 3 $Re_2O_3(PO_4)_2$. Atomic coordinates and displacement parameters. Standard deviations are given in parentheses.

atom	*x*	*y*	*z*	U_{eq} [Å^2] [a]
Re1	1/4	0.5522(4)	0.2865(2)	0.0084(1)
Re2	1/4	0.2430(0)	-0.0292(2)	0.0068(1)
P1	1/4	0.3765(2)	-0.2387(1)	0.0076(3)
P2	1/4	0.6406(2)	0.0665(1)	0.0064(3)
O1	1/4	0.7543(8)	-0.1675(4)	0.0206(16)
O2	1/4	0.4343(7)	0.3908(4)	0.0097(11)
O3	1/4	0.3099(8)	0.2311(4)	0.0122(12)
O4	1/4	0.3941(7)	-0.1393(3)	0.0135(13)
O5	1/4	0.1163(8)	0.0587(4	0.0146(13)
O6	1/4	0.6386(8)	0.1657(4)	0.0157(13)
O7	1/4	0.4574(9)	0.0346(5)	0.0400(28)
O8	0.4416(8)	0.4725(6)	-0.2774(3)	0.0142(9)
O9	0.0606(10)	0.7396(8)	0.0324(3)	0.0297(15)

Table 4 Selected interatomic distances (Å) and angles (°) for $Re_2O_3(PO_4)_2$. Standard deviations are given in parentheses.

d(Re1-O1$_t$)	1.662(6)	*d*(Re2-O5$_t$)	1.667(6)
d(Re1-O2$_b$)	1.838(6)	*d*(Re2-O2$_b$)	1.844(5)
d(Re1-O8) 2x	1.957(5)	*d*(Re2-O7)	1.935(7)
d(Re1-O6)	1.964(6)	*d*(Re2-O9) 2x	1.961(6)
d(Re1-O3)	2.070(6)	*d*(Re2-O4)	2.053(6)
∠(Re1,O2,Re2)	161.4(4)		
d(P1-O3)	1.524(6)	*d*(P2-O7)	1.508(7)
d(P1-O4)	1.525(6)	*d*(P2-O9) 2x	1.513(5)
d(P1-O8) 2x	1.537(5)	*d*(P2-O6)	1.515(6)
∠(Re1,O6,P2)	160.5(4)	∠(Re2,O4,P1)	139.8(4)
∠(Re1,O8,P1)	139.3(3)	∠(Re2,O7,P2)	168.6(6)
∠(Re1,O3,P1)	138.3(4)	∠(Re2,O9,P2)	146.1(4)

Figures

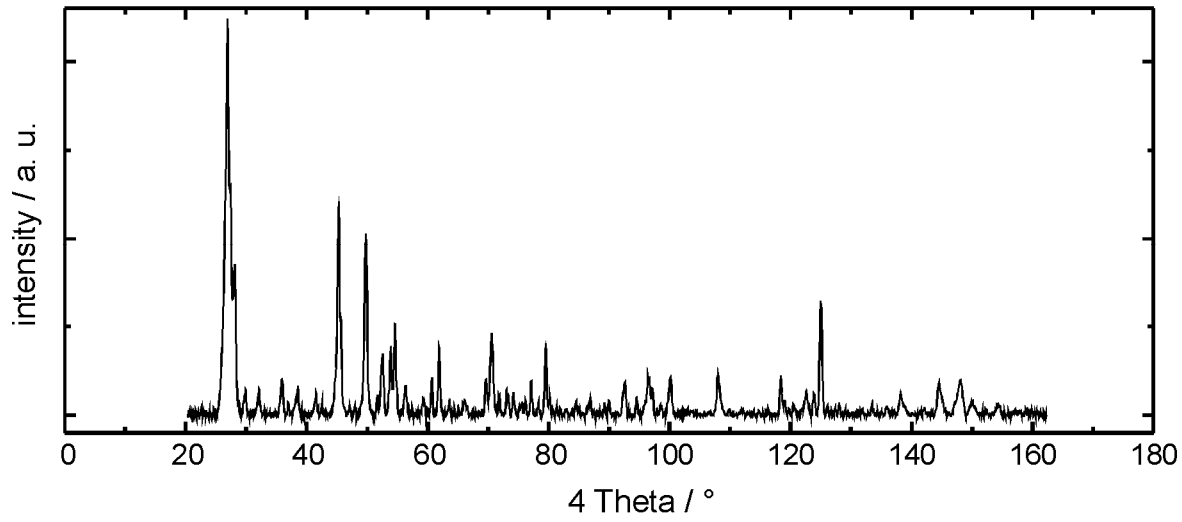

Figure 1 XRPD pattern of "$RePO_6$". *IP* Guinier photograph, Cu-Kα_1.

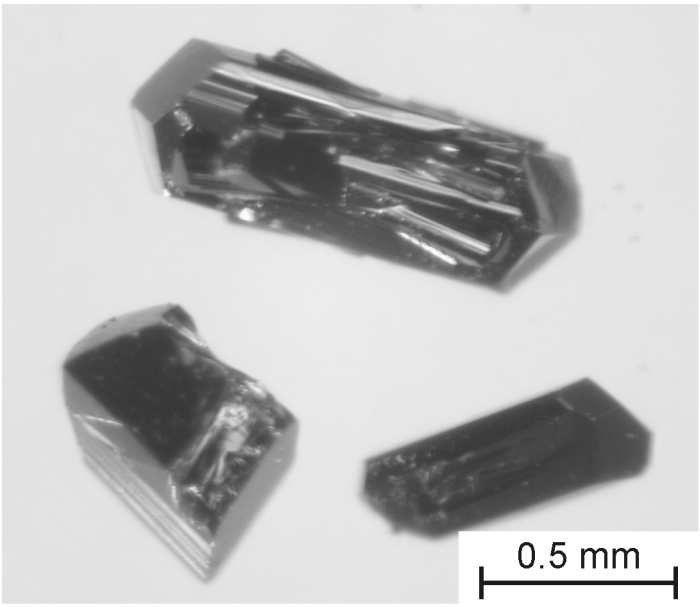

Figure 2 Crystals of $Re_2O_3(PO_4)_2$ obtained by chemical vapour transport.

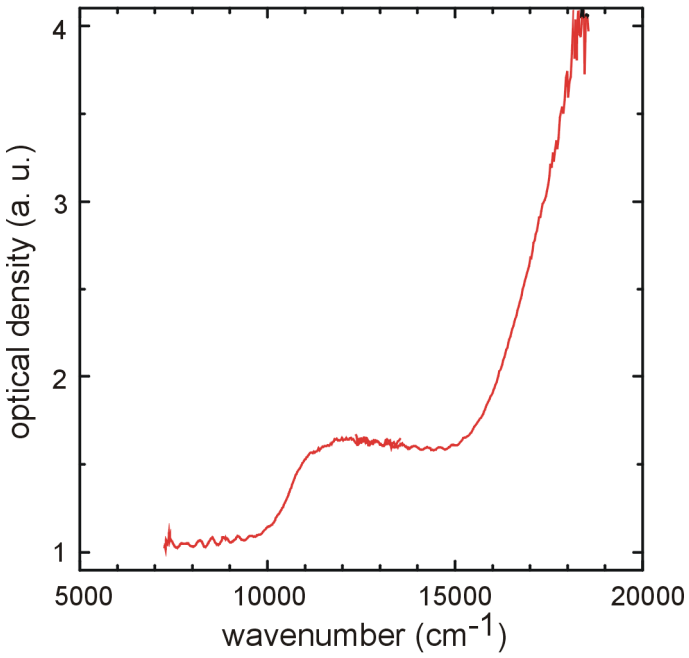

Figure 3 Electronic absorption spectrum of $Re_2O_3(PO_4)_2$.

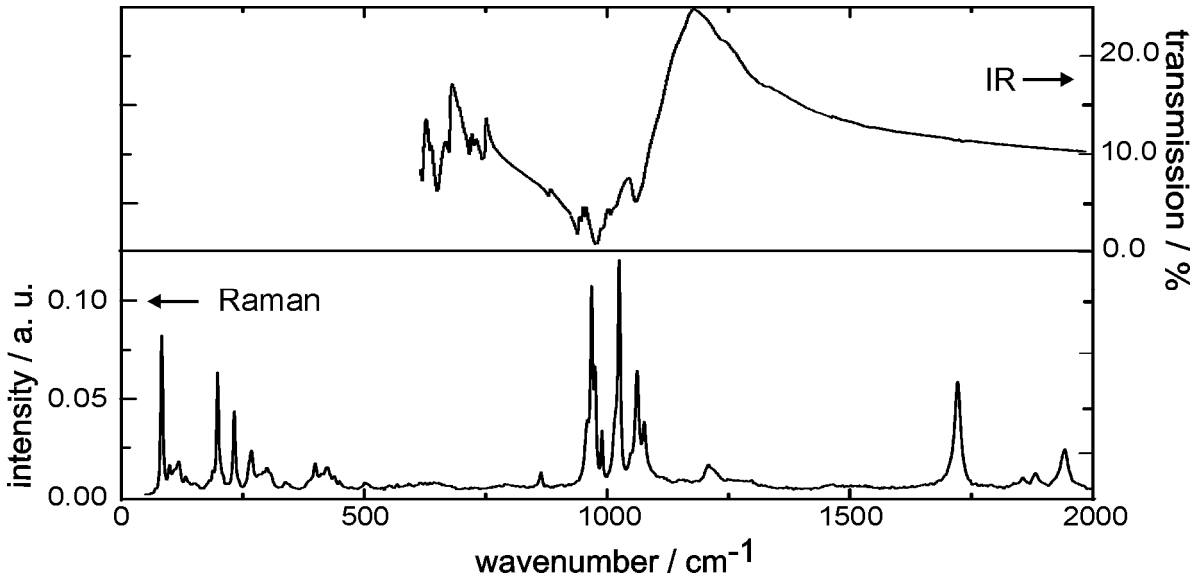

Figure 4 Vibrational spectra of $Re_2O_3(PO_4)_2$.

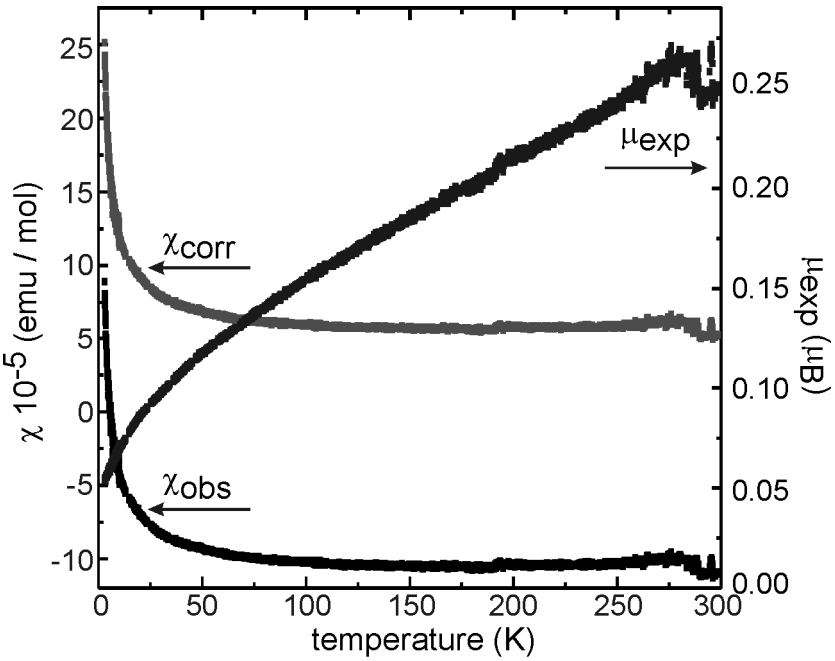

Figure 5 $Re_2O_3(PO_4)_2$. Magnetic susceptibility χ vs. T and magnetic moment μ vs. T.

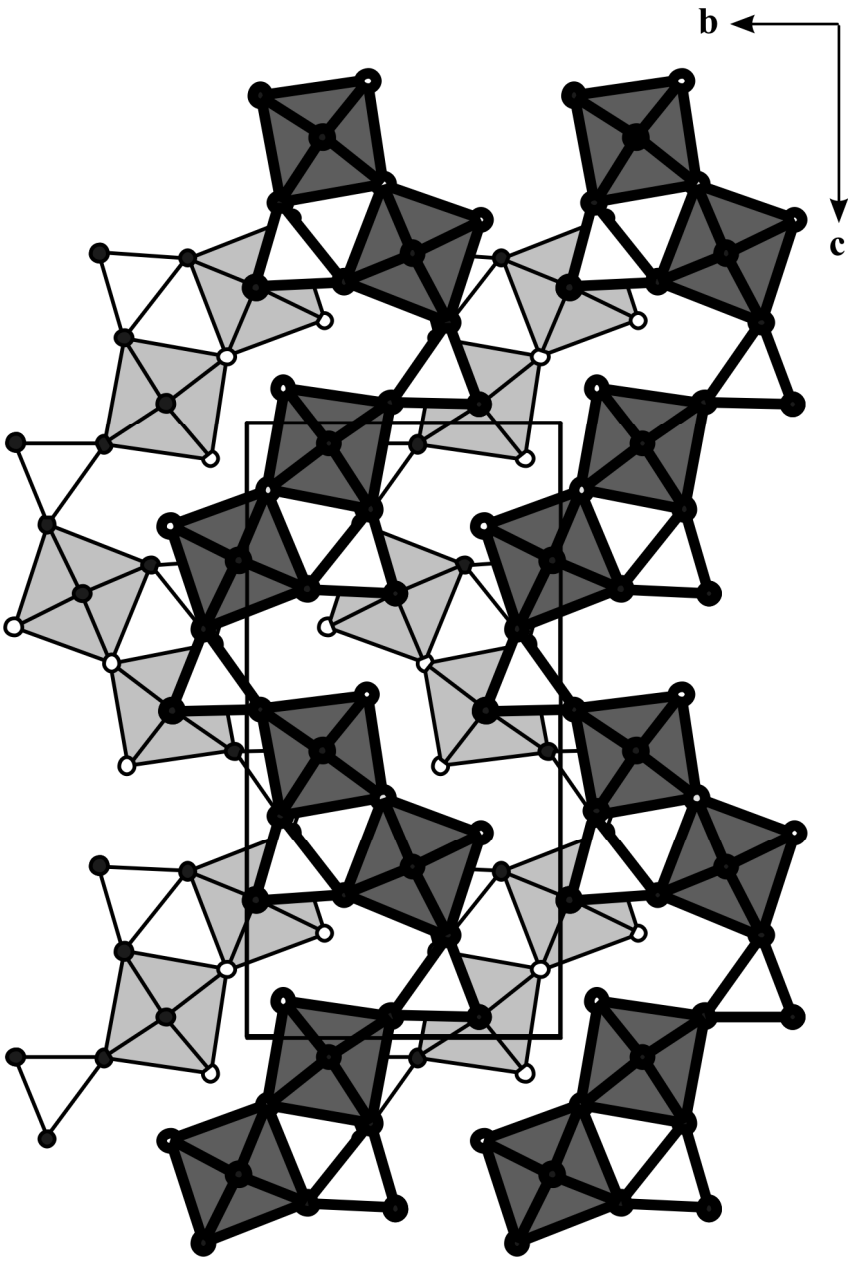

Figure 6 Crystal structure of $Re_2O_3(PO_4)_2$ with ribbons of tetrahedra [PO_4] (white) and [Re_2O_{11}] double-octahedra (grey). Bold lines: polyhedra at x = 3/4, thin lines: polyhedra at x = 1/4. Open circles represent oxygen atoms connected to rhenium only.

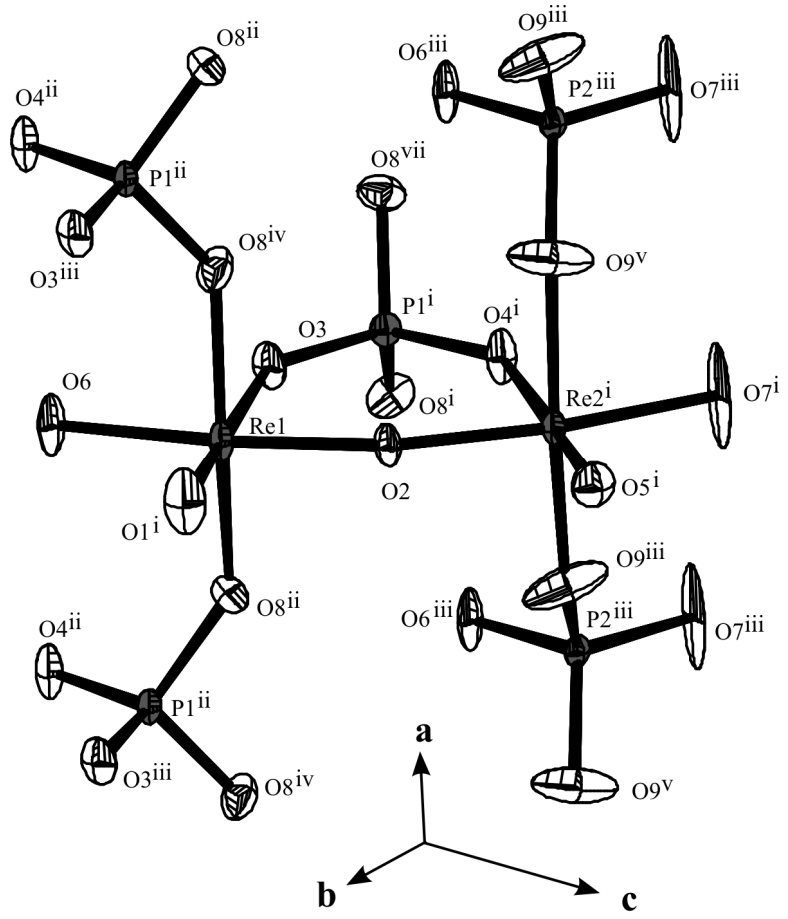

Figure 7 $Re_2O_3(PO_4)_2$**.** ORTEP of the $[PO_4]$ and $[Re_2O_{11}]$ groups. Ellipsoids with 70% probability.

References

[1] Contribution XXXXII in this series: K. Panagiotidis, R. Glaum, W. Hoffbauer, J. Weber und J. Schmedt auf der Günne, *Z. Anorg. Allg. Chem*. **2008**, *634*, 2922.

[2] S. M. Islam, *part of planned Ph.D. thesis*, Univ. of Bonn.

[3] P. Kierkegaard, *Arkiv Kem.* **1962**, *19*, 1.

[4] P. Kierkegaard, *Arkiv Kem*. **1961**, *18*, 521.

[5] P. Kierkegaard, J. M. Longo, *Acta Chem. Scand*. **1970**, *24*, 427.

[6] M. Lenz, *Ph.D. Thesis*, Univ. of Gießen, **1995**.

[7] G. Costentin, A. Leclaire, M. M. Borel, A. Grandin, B. Raveau, *Z. Kristallogr*. **1992**, *201*, 53.

[8] V. V. Lisnyak, N. V. Stus', P. Popovich, D. A. Stratiychuk, Ya. Filinchuk, V. M. Davydov, *J. Alloys Compd*. **2003**, *360*, 81.

[9] A. Leclaire, M. M. Borel, A. Grandin, B. Raveau, *European J. Solid State Inorg. Chem*. **1988**, *25*, 323.

[10] I. M. Watson, M. M. Borel. J. Chardon, A. Leclaire, *J. Solid State Chem.* **1994**, *111*, 253.

[11] P. Kierkegaard, S. Asbrink, *Acta Chem. Scand*. **1964**, *18*, 2329.

[12] M. Hanawa, H. Imoto, *J. Solid State Chem.* **1999**, *144*, 325.

[13] P. Kierkegaard, *Acta Chem. Scand*. **1958**, *12*, 1715.

[14] S. L. Wang, C. C. Wang, K. H. Lii, *J. Solid State Chem*. **1989**, *82,* 298.

[15] A. Leclaire, J. Chardon, B. Raveau, *J. Solid State Chem.* **2000**, *155,* 112.

[16] V. V. Lisnyak, N. V. Stus', N. S. Slobodyanik, N. M. Belyavina, V. Ya. Markiv, J. Alloys Compd. **2000**, *309*, 83.

[17] P. Roussel, P. Labbé, D. Groult, *Acta Cryst*. **2000**, *B56***,** 317.

[18] H. Mathis, R. Glaum, R. Gruehn, *Acta Chem. Scand*. **1991**, *45,* 781.

[19] R. Glaum, *Neue Untersuchungen an wasserfreien Phosphaten der Übergangsmetalle*, Thesis of Habilitation (in German), Univ. of Gießen 1999. URL: http://bibd.uni-giessen.de/ghtm/1999/uni/h990001.htm

[20] E. Banks, R. Sacks, *Mater. Res. Bull*. **1982**, *17*, 1053.

[21] K. Popa, V. Brandel, A. Cecal, *Revue Roumaine de Chem.* **2001**, *46,* 509.

[22] A. Magnéli, *Acta Chem. Scand*. **1957**, *11*, 28.

[23] K. Meisel, *Z. Anorg. Allg. Chem*. **1932**, *207,* 121.

[24] W. Jeitschko, A. W. Sleight, *J. Solid State Chem.* **1972**, *4,* 324.

[25] T. Hartmann, H. Ehrenberg, G Miehe, T. Buhrmester, G. Wltschek, J Galy, H. Fuess, *J. Solid State Chem.* **2001**, *160*, 317.

[26] B. Krebs, A. Müller, H. H. Beyer, *Inorg.Chem*. **1969**, *8*, 436.

[27] R. Glaum, E. Benser, H. Hibst, *Chem. Ing. Tech.* **2007**, *79*, 843.

[28] K. V. Narayana, A. Martina, B. Luecke, M. Belmans, F. Boers, D. van Deynse, *Z. Anorg. Allg. Chem.* **2005**, *631*, 25.

[29] B. K. Hodnett, *Heterogenous Catalytic Oxidation*, John Wiley & Sons, Chichester, **2000**.

[30] H. Schäfer, *Z. Anorg. Allg. Chem.* **1973**, *400*, 253.

[31] H. Oppermann, *Z. Anorg. Allg. Chem*. **1985**, *523*, 135.

[32] L. Reimer, *Scanning Electron Microscopy*, Springer-Verlag, **1983**.

[33] D. Newbury et al., *Advanced Scanning Electron Microscopy and X-ray Microanalysis*, Plenum Press, **1987**.

[34] BASREADER V. 2.26, Program for Windows, Raytest Isotopenmessgeräte GmbH, Straubenhard/Germany, 1999.

[35] AIDA – Advanced Image Data Analyzer (Crystallography) V. 2.02, Raytest Isotopenmessgeräte GmbH, Straubenhard/Germany, 1999.

[36] Y. Amemiya, J. Miyahara, *Nature*, **1988**, *336*, 89.

[37] I. Tanaka, M. Yao, M. Suzuki, K. Hikichi, *J. Appl. Cryst.* **1990**, *23*, 334.

[38] K. Maaß, R. Glaum, R. Gruehn, *Z. Anorg. Allg. Chem*. **2002**, *628*, 1663.

[39] M. Sheldrick, "SHELX-97 (Includes SHELXS97, SHELXL97, CIFTAB). Programs for crystal structure analysis (Release 97-2)", Univ. of Göttingen, Göttingen, Germany, **1998**.

[40] L. J. Farrugia*, J. Appl. Cryst*. **1990**, *70*, 837.

[41] E. Krausz, *AOS News* **1998**, *12*, 21.

[42] E. Krausz, *Aust. J. Chem*. **1993**, *46*, 1041.

[43] W. Klemm, *Magnetochemie*, Akademische Verlagsgesellschaft, Leipzig, **1936**.

[44] W. Klemm, *Z. Anorg. Allg. Chem.* **1941**, *246*, 347.

[45] A. Weiss, H. Witte, *Magnetochemie*, Verlag Chemie, Weinheim, **1973**.

[46] H. Schäfer, *Chemical Transport Reactions*, Acad. Press, New York, **1964**.

[47] R. Gruehn, R. Glaum*, Angew. Chem*. **2000**, *112*, 706; *Angew. Chem. Int. Ed*. **2000**, *39,* 692.

[48] Hk. Müller-Buschbaum, *Z. Anorg. Allg. Chem.* **2007**, *633*, 2491.

[49] M.-R. Lee, *Compt. Rend. Hebd. Acad. Sci., Sci. Chim.* **1970**, *271*, 127. Re2V2O11

[50] A. R. Middleton, A. F. Masters, G. Wilkinson, *J. Chem. Soc. Dalton* **1979**, 542.

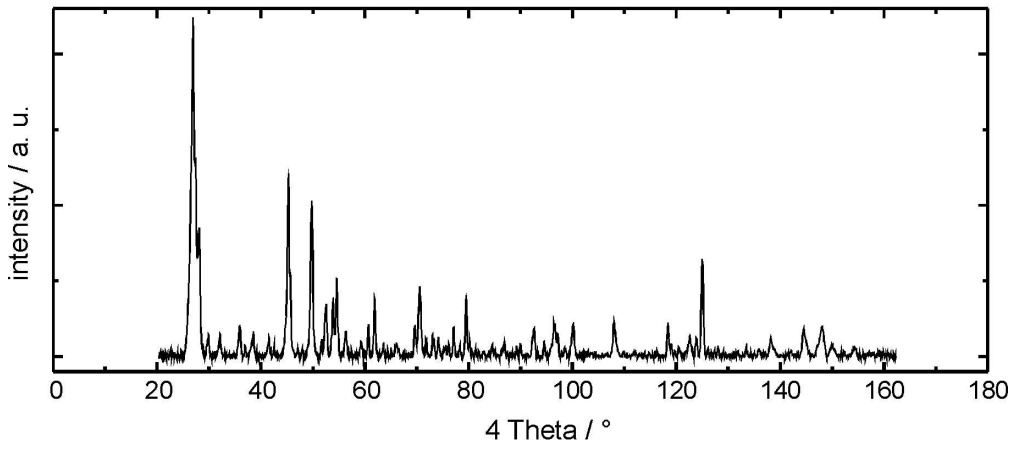

154x70mm (300 x 300 DPI)

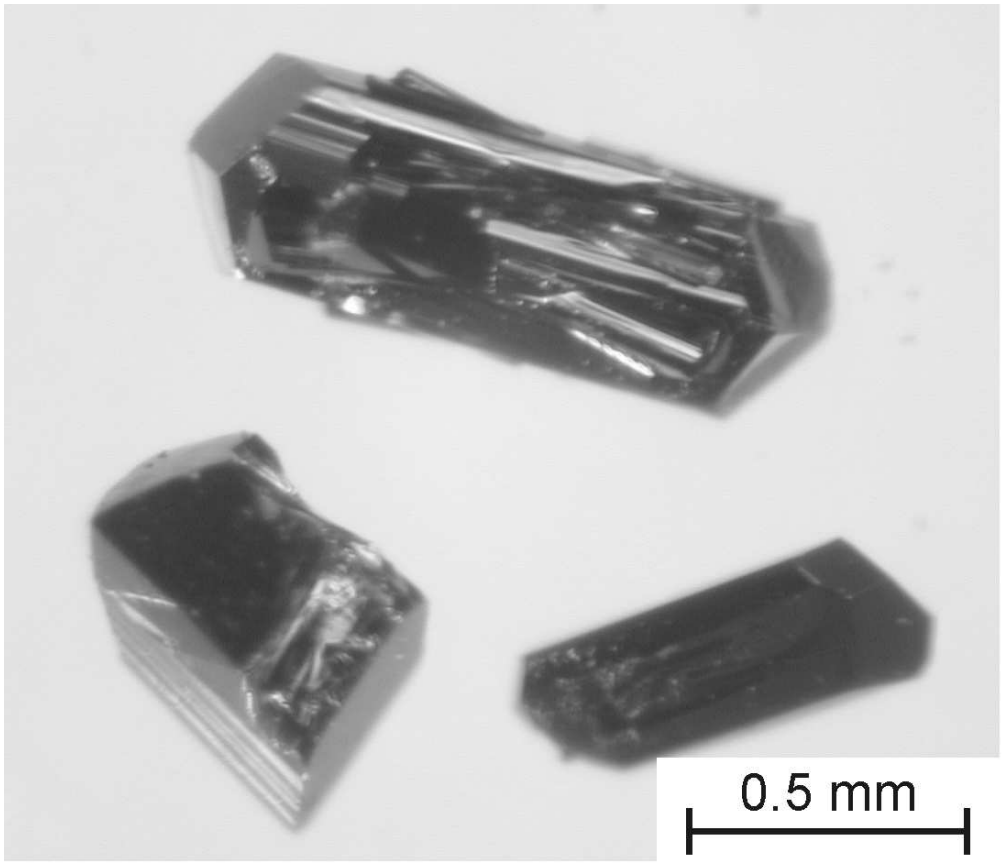

92x79mm (300 x 300 DPI)

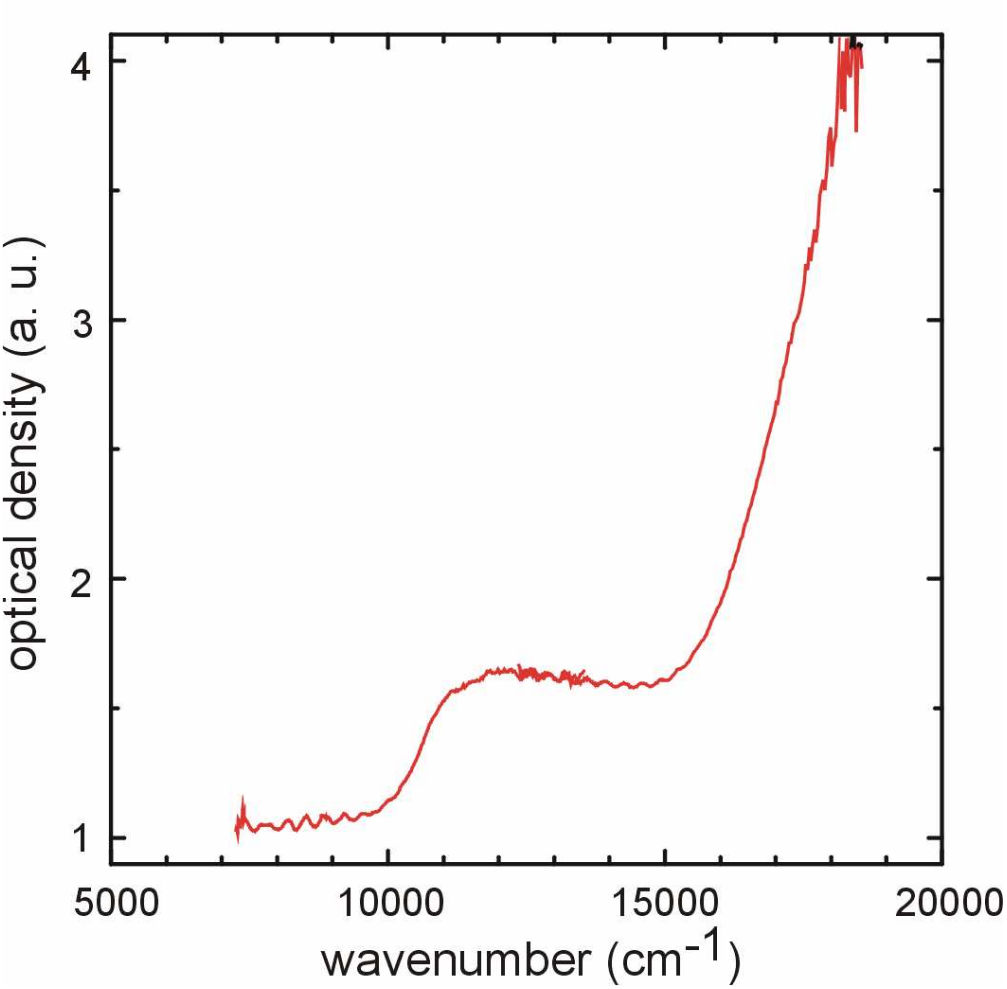
optical density (a. u.)
1
2
3
4
5000
10000
15000
20000
wavenumber (cm-1)

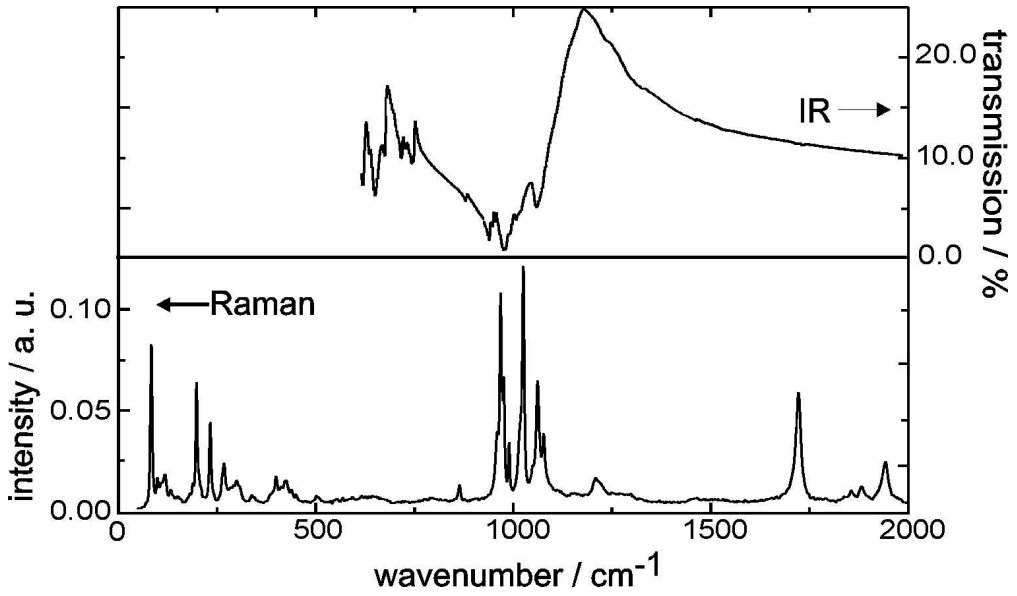

128x74mm (300 x 300 DPI)

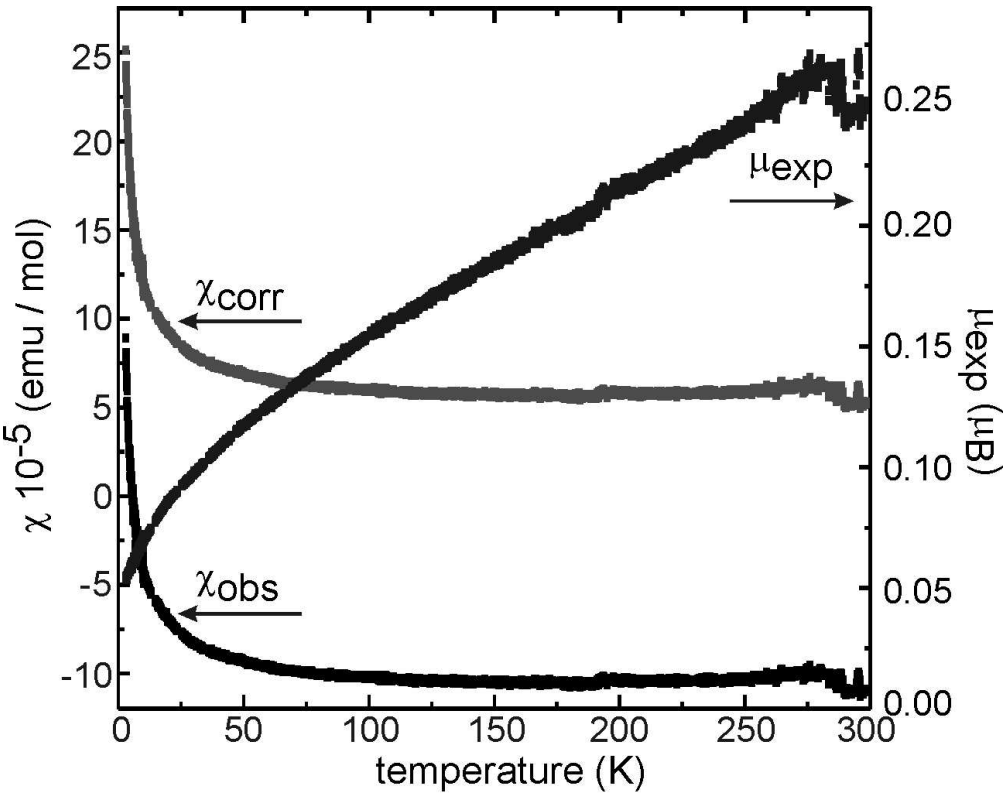

109x86mm (300 x 300 DPI)

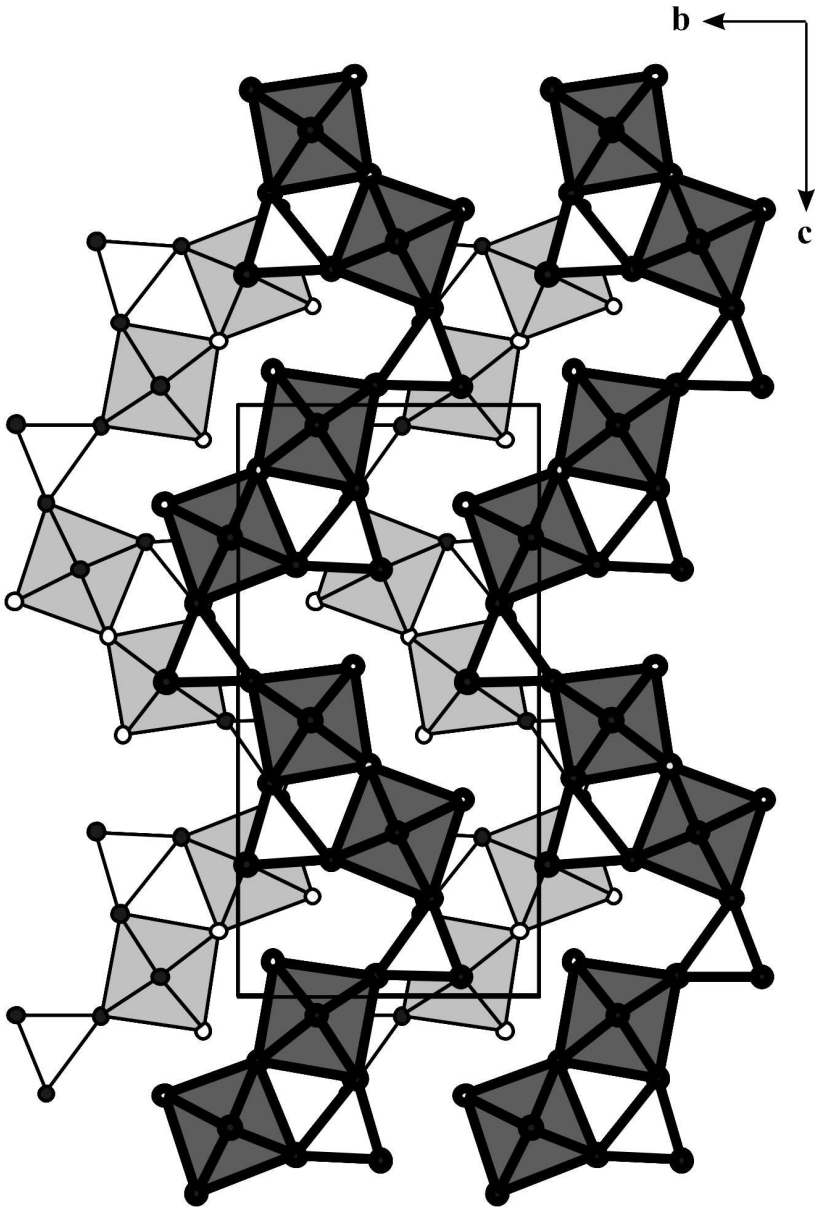

111x164mm (300 x 300 DPI)

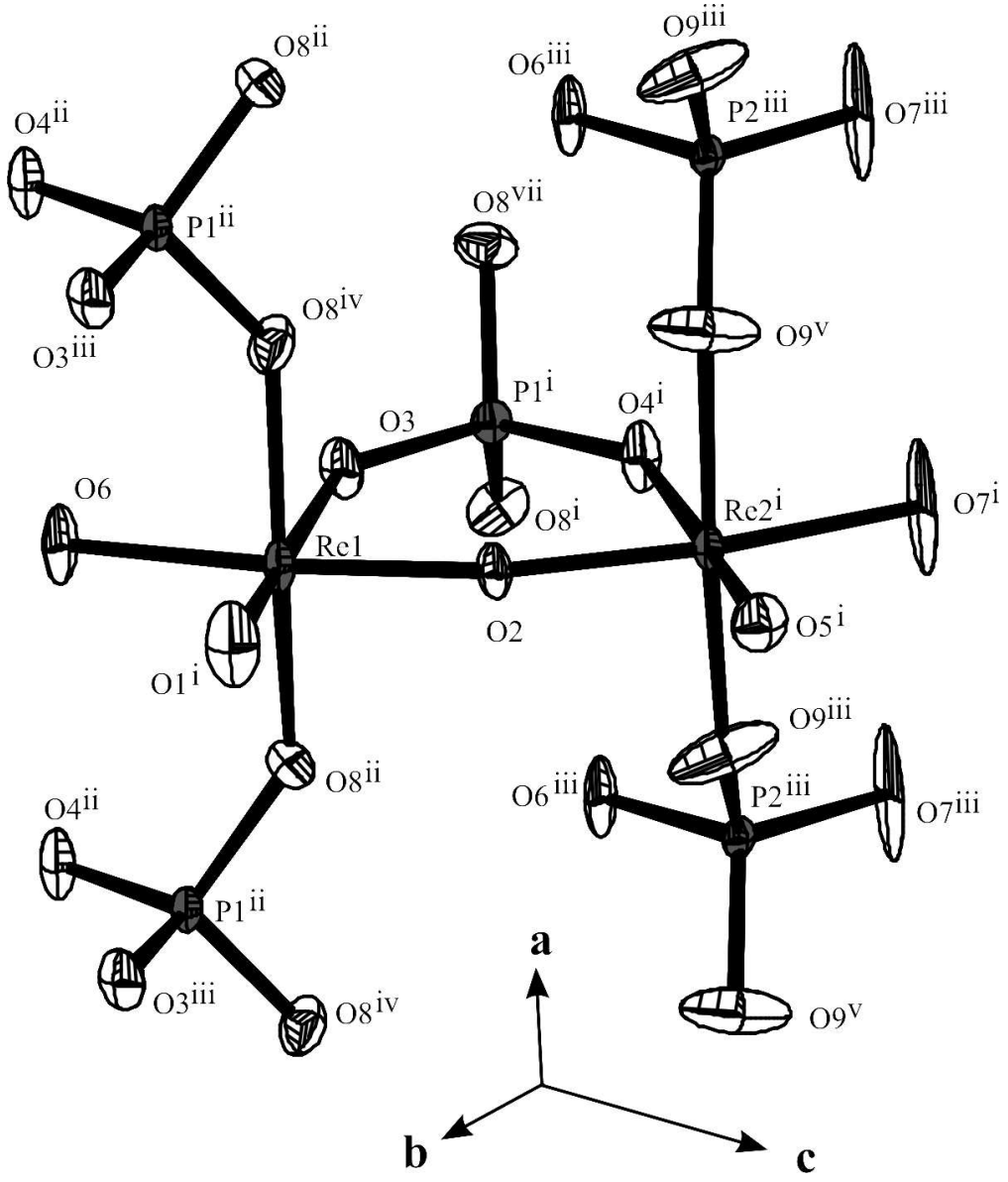

101x119mm (300 x 300 DPI)